J Inno Sci Eng, 2025, 9(1):134-153
DOI:https://doi.org/ 10.38088/jise.1614320
Research Article

Wave Actions and Responses for Large-Diameter Monopod Platform Structures

Ali Ete [1*]

[1] *Istanbul Esenyurt University, Department of Civil Engineering,* 34517, *Istanbul, Turkey*

ARTICLE INFO

Received Date: 6/01/2025
Accepted Date: 16/04/2025

Cite this paper as:
Ete Ali (2025). *Wave Actions and Responses for Large-Diameter Monopod Platform Structures.* Journal of Innovative Science and Engineering. 9(1): 134-153

*Corresponding author: Ete Ali
E-mail:alietemadi@esenyurt.edu.tr

Keywords:
Offshore Structure
Monopod Platform
Morison Equation
Linear Airy's wave theory
Sea-wave loads
Hydrodynamic module
Commercial offshore software

ABSTRACT

The sea-wave loads acting on the fixed offshore structures are estimated by using Airy's linear wave theory and Morison's equation, dissociating the total force into an inertia force component and a drag force component. The contribution of each component of the total force on tubular members can vary significantly based on size specification, from standard pipe members of fixed jacket structures to wide-ranging cylindrical Monopod towers. Inconclusive results can be seen in some published articles in estimating static wave loads using the hydrodynamic module of offshore platforms, indicating that this is still a subject of investigation. A demonstration of an example steel Monopod under Airy's type wave loading is presented. Several finite element offshore structure simulation packages use this simple monopod model for computationally efficient static wave load case simulations. The displacement pattern and the base shear force and bending moment of the Monopod model are calculated. The analytical solution is checked with numerical results of standard commercial FE software packages for verification and comparison purposes. The results show that the wave load calculation module of the finite element-based design programs considered in this study is underestimated, mainly when the contribution of the inertia coefficient to total instantaneous wave force is dominant, like in the monopod case with a large diameter. It can be thought that the differences here are due to the inertia coefficient weighting of the Morrison equation used in wave force calculations.

1. Introduction

Offshore platforms may have one, three, and so forth caisson-type legs. Offshore platforms with an individual caisson-type leg go by the Monopod tower [1]. Monopod steel towers may be applied for observatory, exploration, exploitation, and production aims. It may be appropriate in some offshore regions with shallow or medium seawater depths as a traditional structural concept. They are exposed to specific environmental loads throughout their service life. These loads are forced upon the Monopod tower through natural events such as ultimate wave loading, current, winds, and strong ground motions. For most towers, template, gravity, and caisson offshore structures, the hydrodynamic design load is mainly from sea waves, while wind loads and currents play a minor part [2]. Therefore, safe wave loading estimation is crucial for an economical and reliable design [3-4]. Figure 1 depicts the view of storm waves crashing against the steel Monopod tower.

Figure 1. Monopod tower under storm conditions [5]

While examining wave loads, the sea consists of periodic wave components with various wave heights, wave periods, and traveling ways co-occurring in a particular region. The superposition of these wave components and their distributive action causes a randomly changing sea level height, which can be refined with statistical operations. However, the use of regular wave theories to provide engineering solutions predominates because regular wave theories give well-mathematical models of long-crested periodic waves, which are components of irregular sea waves [6]. There are various regular sea wave theories, going back to the linear Airy's wave theory until the high-order solutions. The linear Airy's wave and Stokes second-order and Stokes fifth-order theories provided good compatibility for engineering applications [7-8].

The evaluation of wave loads on large-diameter vertical cylinders like Monopod is always of great interest to designers, especially now that this type of research is linked to the need to build stable offshore structures in conjunction with oil and gas production [7–18]. Wave kinematics are developed by using Airy's wave theory and Morison's equation. Linton and Evans [9] presented the method assuming linear wave theory for evaluating responses such as the forces on the cylinders, which is much simpler. Kriebel [10–11] developed a closed-form solution for the velocity potential due to the interactive relation of wave theories with a vertical cylindrical component with a large diameter and then compared the theoretical solutions with the results of laboratory experiments. To figure out the overall support size for an offshore platform, it is essential to quickly and accurately estimate the hydrodynamic forces and bending moments. Linear Airy's wave theory and Morison's Equation can be applied for this purpose [19]. Therefore, the wave loads on the large-diameter cylinder can be estimated analytically, and then the design parameters can be plotted in look-up graphs to speed up the design process [13]. Mendes [20] presented a numerical model to predict wave loading on jacket platforms subjected to an incident, regular sea waves. The linear wave theory has been applied to assessing water-particle kinematics. The hydrodynamic forces are enhanced with wave height and the combined effect of sea waves and current.

Furthermore, it was seen that at substantial current velocities, the wave loading is governed by the drag component in comparison with the inertia component. Lipsett [21] presented the impacts of nonlinear drag force on responses of the structure under random sea waves with a steady wave velocity component and a zero mean wave velocity. The wave load was supposed to be given by the relative velocity expression of Morison's equation which links the wave load to the structure's response. Gudmestad and Moe [22] checked the API's regulation and North Sea design practice methods relating to the excerpting convenient rates for the parameters used in the account of the hydrodynamic forces. Sunder and Connor [23] conducted a sensitivity analysis on offshore structures by taking into account different parameters, including alterations in wave height, ambiguities in wave period to be related to wave height; the selection of the hydrodynamic force coefficients, especially in connection with marine growth; modifications in characterizations of offshore structure as well as deck mass. The impacts of different wave patterns on offshore support structures become significant considerations in the hydrodynamic analysis process. The efficacy of hydrodynamic coefficients on response behaviour is connected with wave height and wave period [24-26].

Some studies on numerical modelling for the prediction of wave loading via commercial finite element offshore structure analysis software have been supplied in recent decades. Among them, the SAPOS (Spectral Analysis Program of Structures, [27]), CSI SAP2000 [28], Structural Analysis Computer System (SACS) [29], ABAQUS/AQUA [30], and ANSYS/AQWA [31] are commonly used for hydrodynamic analysis more than other commercial software packages. The hydrodynamic analysis of fixed offshore structure exposed to wave forces using CSI SAP2000 [3, 7, 18, 32-36]; SACS [37-38]; SAPOS [7, 27, 39]; ANSYS [36, 40] and ABAQUS AQUA [41-43] are some examples published by numerous researchers in the recent years. Some of these related studies are listed as follows:

Hydrodynamic analysis of jacket-type substructure for offshore wind turbines subjected to ultimate environmental loads was investigated by using CSI SAP 2000 [32, 34–35]. Environmental loads, such as wave and wind loads for Airy's and Stoke's laws, have been used to calculate offshore structures' deformation demands and bending moments. Cermelli [32] used SAP2000 software to figure out how much the structure of the wind float platform would be stressed when it was built. For the finite element model to work, the force results from the case studies, especially the base shear and overturning moments, had to be changed in a certain way. Raheem [3] showed a nonlinear response analysis for jacket structures under wave loading. The time-dependent wave load was considered through the drag component and the inertia component of Airy's wave theory. The drag force component is dependent upon 2nd-order water particle velocity, and the nonlinearity owing to the wave force has been subsumed in the calculations. Under both regular and extreme waves, the dynamic response of fixed offshore structures was studied, as well as the distribution of displacement demand, bending moment along the leg, and hydrodynamic loading on tubular members. Doman [34] performed a 3D static calculation and design process for a floating platform to support offshore wind turbines. The CSI SAP 2000 software was adopted for response behaviour when the structure was subjected to extreme environmental loads. Das and Janardhan [44] predicted the performance of a typical jacket-type structure at the Mumbai High Basin, using the CSI SAP2000 platform. Slake [18] investigated the effect of wave theories on the dynamic response of the fixed jacket platform. The modelling methods are initially indicated on a simple cantilever column, and then they are utilized for a complex offshore structure of interest (Martin Linge Jacket) on the Norwegian Continental Shelf (NCS).

The wave loading analysis was conducted on a simple beam in advance. Linear Airy's wave theory was employed, and implications were matched with analytical solutions. Airy's wave load on the member was acquired based on Morison's equation. Then, wave loading was developed automatically on the vertical cantilever column. It was conducted to examine the effects of wave loadings through different wave theories and also to verify the SAP2000 FE software results with analytical solutions for the linear Airy's wave theory. Only drag forces for the simple column were calculated manually and compared with the total wave load found from SAP 2000. It is known that the significant contribution comes from drag forces for slender members, such as members of jacket structures. The contribution of inertia forces should have been addressed in simple column calculations, which is not the case for vertical cylinders with a large diameter, such as monopod towers.

ANSYS/AQWA, ABAQUS/AQUA, and Structural Analysis Computer System (SACS) software have a workbench interface and direct use of the finite element analysis (FEA) solver dealing with offshore structures submitted to sea wave loads. Based on ABAQUS/AQUA environment, a steady current, Airy's wave load, and loads due to drag, buoyancy, and inertia forces for certain rigid elements can be defined easily [43]. Dagli et al. [45] investigated the bi-directional fluid-structure interaction analysis of monopod towers subjected to surface wave loads. Yaylacı [40] presented an offshore structure and its material properties in the examples using ANSYS software. Wave loads impacting a jacket structure were defined on the model and solved for multiple design scenarios. Kazemi Daliri [36] conducted time domain analysis on a gas/oil export riser subjected to wave loads using ANSYS/AQWA software. The risers have been assumed to be situated in a fixed jacket structure settled in the North Sea. The nodal displacements and reaction forces were compared by using different wave-loading theories. Noorzaei [37] presented the analytical solution and introduced an analysis platform to develop wave and current loads of slender offshore members. The developed program's results matched those of the Structural Analysis Computer System (SACS) software. Ishwarya [38] performed the nonlinear static and dynamic analyses on a three-dimensional model of a fixed jacket structure for North Sea environments, using the SACS platform.

In this research, commercial programs' static wave load calculation is examined through a simple benchmark monopod tower problem with a large diameter. The solution is compared with numerical results. The parameters used in the calculations are not real engineering design examples, and the structure size and wave load properties are hypothetical values for this study. The static sea wave forces applied on the Monopod tower are calculated through Morison's equation, which dissociates the overall wave force into an inertia force component that changes linearly with the water particle acceleration and a drag force component that changes quadratically with the water particle velocity. The Monopod tower under Airy's wave loads is solved manually by Morison's equation. Finite element models are formulated to designate the internal forces and displacements under similar wave loadings. The contribution of inertia and drag components on the total wave was calculated theoretically for comparison with the finite element method results. Commercial software packages, including SAPOS, SACS, SAP2000, and ABAQUS AQUA, are applied to calculate sea wave loads in the Monopod tower. The results of these examinations emphasize the stature of accurately simulating wave loading in cylindrical members with large diameters from the view of wave load prediction and safe design. Briefly, the primary aim of this research is to (i) compare the analytical results with the numerical solution of commercial finite element-based programs that can model wave forces on Monopod tower using Airy's wave theory and (ii) to demonstrate the applicability of the wave load module by analyzing a simple cylindrical Monopod tower instead of a complex offshore structure for the simplicity of comparison between the analytical solutions and numerical results.

2. Model design description and wave load data

The cylindrical monopod tower with a large diameter is adopted to compute static sea wave loads using Airy's linear wave theory and Morison's equation. The vertical steel Monopod tower with a diameter of 15.0 m is installed at a site where the water depth is 100 m. The height of the tower is 120.0 m. The monopod tubular section is made of welded plates with 0.08 m thickness. The steel material used for the construction of this platform is S355. Model design description, material properties, and Airy's wave load data are listed in Table 1. Considering the water-structure interaction, the added mass is assigned to the Monopod tower, concerning the added mass coefficients. A mass numerically equal to the mass of water displaced by the submerged monopod part is utilized to contain marine growth where practicable. Table 1 includes the added mass coefficients in dependence upon submergence, the thickness of marine growth, and the dry density of marine growth. D_h is the tower diameter containing marine growths, i.e., $(D_h = D + 2h)$ where h is the thickness of marine growths and D is the diameter of the member. The mean current defines a changing pressure distribution around the Monopod, producing a steady drag force on the cylindrical Monopod tower in line with the flow neglected in this study. The weight of the deck is not considered in the hydrodynamic analysis. The buoyancy force assigns to the Monopod tower water in the reverse direction of the gravitational loads. This force is ignored in the analysis. The soil-pile interaction effect is neglected. A regular periodic waveform is illustrated in Figure 2. The design wave has a height of 2.5 m and a wave period of 6.5 s. A schematic Monopod tower, geometry and material definition, and wave load data are summarized in the figure. The monopod tower was divided into 20-meter pieces starting from the seabed, then into elements 3-5 of 10 meters in length, 5-meter elements for the 30-meter piece at sea depth, and finally into 2 pieces 20 meters above the water level, thus obtaining a total of 14 elements. Detailed information on the number of elements and nodes for all models is presented in Figure 2. θ is the direction angle of the individual wave propagation and is defined between $(-\pi / 2 \leq \theta \leq \pi / 2)$ [7]. For regular waves, the wave amplitude $\hat{\eta}$ is to the halving of the wave height, $H/2$. Other dependent wave profile parameters can be calculated by using the data in Table 1. The wave number $m = 2\pi/\lambda$ and the other dependent parameters are angular wave frequency, $\omega = 2\pi/T$, and wave steepness, $\alpha = H/\lambda$ and wave celerity, $C = \lambda/T = \omega/m$.

Despite the dynamic nature of wave loads, they can be efficiently symbolized by their static equivalents to quasi-static loads. According to Morison's Equation, the force exerted by unbroken surface waves on a monopod tower has two components, inertia and drag forces [19]. Due to the wave forces, the members experienced stress depending on time, thus contributing to the cantilever impact as a deflection on the monopod towers. The solution to Morrison's equivalent forces for the Monopod tower example is presented in the following section.

Table 1: Model design description, material properties, and wave load data

Model Description		
Parameters	**Designation**	**Value (Unit)**
h_s	Height of the tower	120.0 (m)
D	Diameter of the tower	15.0 (m)
t	Wall thickness of the tower	0.08 (m)
Material properties		
ρ	Steel Mass Density	$7800.0\ (kg/m^3)$
ν	Poisson's ratio	0.30
f_y	Yield stress	$450.0 \times 10^6\ (P_a)$
E	Young's Modulus	$205.0 \times 10^9\ (P_a)$
Wave load		
ρ_w	Mass density of the water	$1024.0\ (kg/m^3)$
d_w	Water depth	100.0 (m)
	Still water surface	100.0 (m)
H_{max}	Maximum wave height	2.5 (m)
	wave period	6.5 (s)
C_d	Transverse Drag force Coefficient	1.3
	Tangential Drag force Coefficient	0.0
C_m	Transverse Inertia force Coefficient	2.0
Marine Growth		
	Marine Growth	0.25 (m)
	Dry density of marine growth	$1400\ (kg/m^3)$

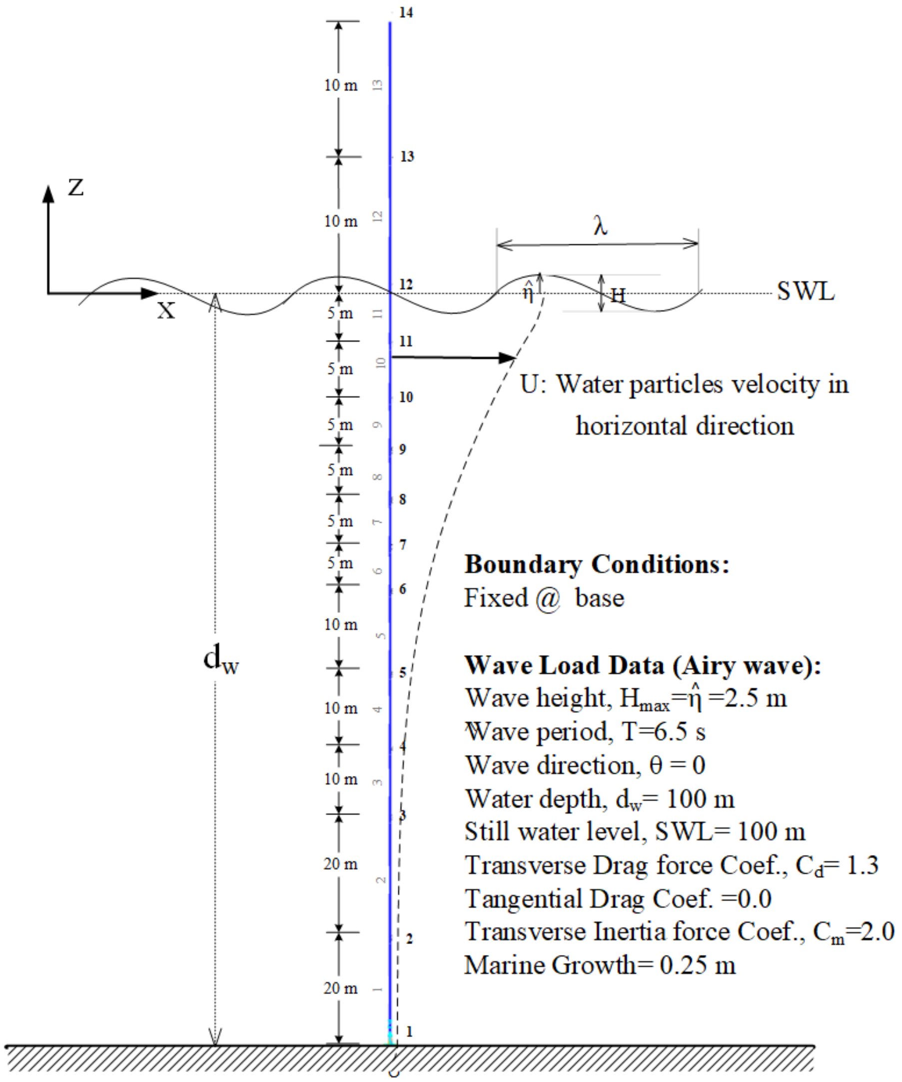

Figure 2. A schematic Monopod tower geometry, two-dimensional waveform, and description of some symbols

3. Analytical solution

Hydrodynamics principles are used to obtain water surface waves under certain boundary conditions from incompressible, irrotational, and inviscid flow [46]. The fundamental equations of water waves that fulfil various boundary conditions at the sea's bottom and on its free surface are continuity and irrotationality conditions of the flow. The linear Airy wave theory is the most straightforward and practical theory amongst wave theories. The assumption of low relative water depth and small wave steepness enables the linearization and satisfaction of the free surface boundary conditions at the still water level (mean water level). Airy's finite and infinite water depth theory calculates to provide an accurate depiction of the fundamental wave force. Then, one can determine Airy's wave force, using Morison's equation [19], which is provided for a rigid cylindrical monopod fixed at the bottom. The Morrison force expression depends on velocity, acceleration, and time, which on its own also depends on the depth considered. As a result, the force was reduced due to a combination of increased drag and added mass coefficients and the decreased absolute value of velocity and acceleration.

The computation of the force that sea waves apply to a cylindrical monopod tower changes depending on the wavelength, λ, and the member's diameter, D. The incident waves are dispersed or diffracted when the size of a cylindrical part is large enough to cover most of a wavelength. It may be in the diffraction regime based on the diameter of the Monopod tower. A solution to the linear diffraction issue for a cylindrical tower expanding from the seabed through the still water level can be found in [7-8, 47-48]. This ratio is not considered in this benchmark problem, and the pressure acting on the monopod due to the scattered wave is not incorporated. Instead, the wave forces have been obtained by using the Morrison equation and by calculating the pressure acting on the monopod tower from incident waves. Morison's equation disregards the convective acceleration component in the calculations of inertia force, slam forces, lift forces, and axial Froude-Krylov forces. According to Eq. 1 [49], Morison's equation, which is parallel to the planes of wave propagation direction and perpendicular to the monopod tower, defines a distributed wave force per unit length.

$$F = F_D + F_I = C_D \cdot |U| \cdot U + C_M \cdot \frac{\delta U}{\delta t} \tag{1}$$

Where F is the whole instantaneous force, the magnitude and direction change during the wave's passage. The drag force contribution (F_D) is the first term, while the inertia force (F_I) is the second. The components of a water particle's velocity and acceleration, U and $\frac{\delta U}{\delta t}$, are normal to the tower axis. $|\cdot|$ designates an absolute value. Eq. 2 defines C_D and C_M, respectively, representing the drag and inertia force constants.

$$\begin{aligned} C_D &= \frac{1}{2} \cdot D_h \cdot \rho_w \cdot C_d \\ C_M &= \frac{1}{4} \cdot \pi \cdot D_h^2 \cdot \rho_w \cdot C_m \end{aligned} \tag{2}$$

Where C_d and C_m are Morison's equation's coefficients for drag and inertia force, respectively and are listed in Table 1. These coefficients depend on the Keulegan-Carpenter number (K_c), which considers wave height and surface roughness, and the Reynolds number (R_e), a dimensionless parameter based on flow velocity. The cylinder's diameter, D_h, has an impact on the wave force regime as well.

By using the linear wave theory, a velocity potential function for two-dimensional waves can be obtained as,

$$\phi = -\hat{\eta} \cdot \frac{g}{\omega} \cdot \frac{\cosh(mz + md_w)}{\text{scosh}(md_w)} e^{i(\omega t - mx)} \tag{3}$$

where,

d_w: Water depth

g : Acceleration of the gravity

m : Wave number ($m = 2\pi/L$ where L is the wavelength)

z : Vertical coordinate measured from the still water level

x : Horizontal coordinate in the wave propagation direction.

The wave number m is also dependent on the frequency ω by the relation,

$$\omega^2 = (mg) \cdot \tanh(m \cdot d_w) \tag{4}$$

The water elevation η and velocities of water particles may be derived from the potential function as written by,

$$\eta = \frac{1}{g}\frac{\partial \phi}{\partial t}|z = 0 \quad \text{and} \quad \begin{aligned} U_x &= -\frac{\partial \phi}{\partial x} \\ U_z &= -\frac{\partial \phi}{\partial z} \end{aligned} \tag{5}$$

Having used the statement of Φ given by Eq. (3) in Eq. (5), the real parts of these quantities will be,

$$\eta = \hat{\eta} \cdot \sin(\omega t - mx) \tag{6}$$

$$U_x = \hat{\eta} \cdot \omega \cdot \frac{\cosh m(z + d_w)}{\sinh(md_w)} \sin(\omega t - mx)$$

$$U_z = \hat{\eta} \cdot \omega \cdot \frac{\sinh m(z + d_w)}{\sinh(md_w)} \cos(\omega t - mx) \tag{7}$$

The accelerations of water particles are derived from Eq. (6) as,

$$\dot{U}_x = \hat{\eta} \cdot \omega^2 \cdot \frac{\cosh m(z + d_w)}{\sinh(md_w)} \cos(\omega t - mx)$$

$$\dot{U}_z = -\hat{\eta} \cdot \omega^2 \cdot \frac{\sinh m(z + d_w)}{\sinh(md_w)} \sin(\omega t - mx) \tag{8}$$

or using Eq. (4) in Eq. (8), it can be obtained as,

$$\dot{U}_x = \hat{\eta} \cdot mg \cdot \frac{\cosh m(z + d_w)}{\cosh(md_w)} \cos(\omega t - mx)$$

$$\dot{U}_z = -\hat{\eta} \cdot mg \cdot \frac{\sinh m(z + d_w)}{\cosh(md_w)} \sin(\omega t - mx) \tag{9}$$

where $m = 2\pi/\lambda$, (λ is the wavelength). Eqs. (7) and (9) will be used in calculation of wave forces from the Morison’s equation. The Morison's equation is used to figure out the wave load on a monopod tower when the wave profile is assumed to be harmonic, as shown in Eq. 10. Also, because the tower response is static, the contribution of the dynamic response is not considered. Under harmonic wave loads, the shear force and bending moment of the monopod tower example at the bottom are determined. The maximum wave-induced horizontal drag force F_D and an inertia force F_I are computed analytically for the values in Table 1 [7]. To calculate the extreme shear force and bending moment of the tower in practice, wave velocity and acceleration, which are based on a finite amplitude wave theory, must be used. For a progressive wave moving in the direction of $+x$, the horizontal velocity vector U of water particles is found using the Eq. 10. For the static analysis, the wave elevation is calculated by using a complex exponential function $\exp(i(\omega t - mx))$ with constant amplitude.

$$U = \hat{\eta} \cdot \omega \cdot \frac{\cosh m(z + d_w)}{\sinh md_w} \tag{10}$$

in which m is a constant (wave number), $\hat{\eta}$ is the wave amplitude and equal to the halving of the wave height $(H/2)$ for regular waves, x_w is the horizontal coordinate in the wave propagation direction, and U is the water velocity in the x_w direction. With velocity data, the Morrison equation [19] can be used to figure out the wave forces on the monopod tower. As shown in Eq. 11, in the first term of Morison's equation, $F_D(z)$ is the drag force per unit length acting on the axis of the monopod tower in the plane of the member axis.

$$F_D(z) = C_D \left(\hat{\eta} \cdot \omega \cdot \frac{\cosh m\,(z + d_w)}{\sinh md_w} \right)^2 \tag{11}$$

The following integration yields the total shear force at the bottom, V_D,

$$V_D = \int_{Z=-d_w}^{0} F_D(z) \cdot dz \tag{12}$$

$F_D(z)$ from Eq. 11 is then substituted into Eq. (12). Giving the derivation from both sides of the $m(z + d) = x$ expression to get $mdz = dx \rightarrow dz = \frac{dx}{m}$ and carrying out the integration for boundary conditions as $= -d \rightarrow x = 0$, $z = 0 \rightarrow x = md$ and substituting them into Eq. 13, the shear force at the bottom is calculated as Eq. 14.

$$V_D = \int_{0}^{md} C_D \cdot \left(\hat{\eta} \cdot \frac{\omega}{\sinh md} \right)^2 \cdot \frac{1}{m} \cdot \cosh^2 x \, dx \tag{13}$$

$$V_D = \frac{1}{4} \cdot \frac{C_D}{m} \cdot \hat{\eta}^2 \cdot \frac{\omega^2}{\sinh^2 md} \cdot \sinh 2md \cdot \left(1 + \frac{2md}{\sinh 2md} \right) \tag{14}$$

where the frequency of the wave, ω, that fulfils the dispersion relationship is $\omega^2 = mg \cdot \tanh md_w = mg \cdot \frac{\sinh md_w}{\cosh md_w}$ and replacing of $\sinh md_w \cdot \cosh md_w = \frac{1}{2} \cdot \sinh 2md_w$ expression into Eq.14, the shear force at the bottom due to drag force is simplified as Eq. 15.

$$V_D = \frac{1}{2} \cdot C_D \cdot g \cdot \hat{\eta}^2 \cdot \left(1 + \frac{2md}{\sinh 2md} \right) \tag{15}$$

The deep-sea wave condition is effectively employed in ocean conditions distant from the shoreline. Waves are divided into the categories of deep, moderate, and shallow water waves based on the connection between water depth and wavelength, d_w/λ, [50]. The deep-water condition is established when $(d_w/\lambda > 1/2)$. The alternative form of this condition is $(md > \pi)$. For the deep-water situation, instead of using Eq. 10, the velocity vector component in Eq. 16 is used. The drag force is formed as in Eq. 17.

$$U = \hat{\eta} \cdot \omega \cdot e^{mz} \tag{16}$$

$$F_D(z) = C_D \cdot \hat{\eta}^2 \cdot \omega^2 \cdot e^{2mz} \tag{17}$$

Eq. 18 is employed to determine the tower's shear force at the base due to drag and deep-water conditions,

$$V_D = C_D \cdot \hat{\eta}^2 \cdot \frac{\omega^2}{2m} \cdot \left(1 - e^{-2md} \right) \tag{18}$$

The following integration yields the bending moment of monopod at the bottom,

$$M_D = \int_{Z=-d}^{0} (d + z) \cdot F_D(z) \cdot dz \tag{19}$$

The bending moment is expressed after $F_D(z)$ in Eq. 17 was added to Eq. 19.

$$M_D = V_D \cdot d + C_D \cdot \hat{\eta}^2 \cdot \omega^2 \cdot \int_{-d}^{0} z \cdot e^{2mz} \cdot dz \tag{20}$$

Moreover, after integration is completed, it is possible to ascertain,

$$M_D = V_D \cdot d + C_D \cdot \hat{\eta}^2 \cdot \frac{g}{m} \cdot [(2md + 1) \cdot e^{-2md} - 1] \tag{21}$$

The constants for the bending moment's drag and inertia terms, B_D and B_M can be expressed more simply as follow,

$$M_D = \frac{g}{m} \cdot \hat{\eta}^2 \cdot B_D \tag{22}$$

where Eq. 23 is used to obtain the constants B_D of the drag force terms,

$$B_D = \frac{1}{4} \cdot C_D \cdot \left[2md - \left(1 - e^{-2md}\right)\right] \tag{23}$$

It is also possible to ignore the term in Eq. 23 for deep water conditions, and the constants for the drag terms of the bending moment at the bottom can be simplified as shown below,

$$B_D = \frac{1}{4} \cdot C_D \cdot (2md - 1) \tag{24}$$

$$\rightarrow \text{for deep water condition}$$

Also, the bending moment is only caused by the inertia force part of the Morison equation forces, M_M, which is found in Eq. 25.

$$M_M = \hat{\eta} \cdot \frac{g}{m} \cdot B_M \tag{25}$$

And the following formula is used to determine the inertia terms' constants B_M,

$$B_M = C_M \cdot \left[md \cdot \tanh(md) + \frac{1}{\cosh(md)} - 1\right] \tag{26}$$

In addition, the constant B_M for the inertia term in the case of deep-water situation is derived as follows,

$$B_M = C_M \cdot (md - 1) \tag{27}$$

→ for deep water condition

Finally, Eq. 28 is used to figure out the shear force that the force of inertia will have on the base of the monopod tower. This is determined in a way like how Eq. 15 describes the shear force brought on by the drag force.

$$V_M = \hat{\eta} \cdot g \cdot (C_M \cdot \tanh(md)) \tag{28}$$

Eqs. (19) and (23) enable us to find the maximum static total shear force and bending moment under the monopod tower for a given wave. Eq. 2 defines C_D and C_M, the drag and inertia force constants, respectively. By substituting the design parameters of the monopod tower according to Table 1, the drag force coefficient is calculated as $C_D = 807.1875$, and the shear force and the bending moment due to the drag force at the bottom of the monopod are calculated as $V_D = 961.036\ kN$, $M_D = 0.6849 \times 10^8\ N \cdot m$, respectively. Moreover, the bending moment due to the inertia force term is obtained as $M_M = 0.20430253 \times 10^8\ N \cdot m$, and the coefficients of the inertia forces are computed as $C_M = 2173.589$ and $B_M = 2408$, respectively.

In deep water, the maximum static bending moment depends on both the number and size of the waves, but the maximum static shear force depends only on the size of the waves [7]. The shear force is obtained as $V_D = 799.209\ kN$ for the tower in question in deep water conditions. The B_D coefficient and the moment forces are found to be equal to $B_D = 530.6148$ and $M_D = 0.6781 \times 10^8\ N \cdot m$, respectively. Furthermore, the moment force due to inertia force and related the B_M coefficient are calculated as $M_M = 0.17323179 \times 10^8\ N \cdot m$ and $B_M = 1952.1$, respectively.

4. Numerical model development

This section generates the finite element (FE) models of the cylindrical steel monopod model. The global FE model is developed through the commercial FE offshore analysis software packages: SAPOS (Spectral Analysis Program of Structures) [27], SAP2000 V.20 [28], Structural Analysis Computer System (SACS) V.12 [29], and ABAQUS V.6.14 [30]. The hydrodynamic analysis of the cylindrical monopod tower under Airy's wave loads is conducted. The shear forces and bending moments at the bottoms are computed numerically, and the results are compared with analytical solutions.

4.1. SAPOS Software

The stochastic analysis program for offshore structures is known as SAPOS [7]. Because the wave amplitude and profile are random, the shear force and static bending moment are calculated and expressed in terms of the random water level. For this reason, the real and imaginary components of the water elevation η have been introduced [7]. Design parameters for monopod tower cases are adopted as per Table 1. The input file for wave loading in the SAPOS program is shown in Table 2. Under Airy's theory of waves and conditions of deep water, the SAPOS reported the forces and displacement demands of the members. The moment at the basement due to inertia and drag forces is computed in Table 3. Based on analytical results, the maximum resultant moment forces at the midline are estimated to be off by 1.5%. The results show that the moment forces from SAPOS and the analytical solutions (see

Table 3) are the same. Figure 3 shows the member forces and nodal displacements calculated from SAPOS for the monopod tower as well as the results for both the imaginary and real parts. The weight of the imaginary part is the most important factor when estimating displacement patterns and the forces at the nodes. It is seen that the results of the analysis using SAPOS are consistent with the analytical solution for the same problem.

Table 2: Input file for wave loading in the SAPOS program

```
WAVe DATA
WAVe HEIght 2.5
WAVe PERiod 6.5
WAVe DIRection 0.0
WATer depth 100.0
STIll water surface 100.0
UNI-directional
MAin wave number 1
INErtia force coefficient cm 2.0 ALL
DRAg force coefficient cd 1.3 ALL
MARine growth thickness 0.25 ALL
DENsity of water ro 1024.0
     END of wave data
```

Table 3: The moment force at the basement

Software	$M_M\ (N \cdot m)$		$M_D (N \cdot m)$	
	Normal condition	Deep water condition	Normal condition	Deep water condition
Analytical solution	0.1732×10^8	0.1732×10^8	-	0.6780×10^8
SAPOS	-	-	-	0.6675×10^8
SAP2000	-	-	-	0.1024×10^8
SACS	-	-	-	0.497×10^7

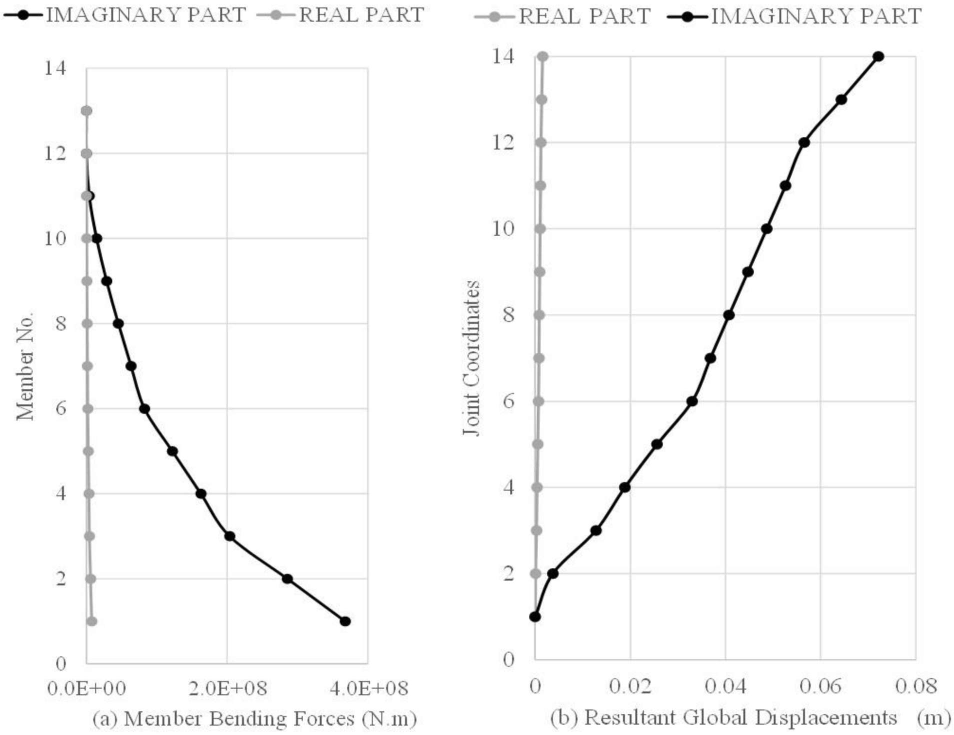

Figure 3. (a) Resultant moment forces (N.m) and (b) Resultant global displacement (m)

4.2. CSI SAP2000 Software

The CSI SAP2000 Ultimate Version 20.1.0 analysis software, which is based on finite elements, is used to perform a first-order elastic analysis on the Monopod tower model [28]. As suggested by [2], the displacement response of the hull structure is found by analysing wave loading cases that take the environmental condition into account. The wave loading results from the water pressure integrated over the submerged part of the monopod tower [51]. The automatic wave loads are based on the requirements for designing fixed offshore platforms given by APR RP 2A-WSD [2]. CSI SAP2000 represents the application of static wave load patterns by a significant wave height, a specified wave return period, and a direction (Figures 4 and 5). Wave velocities and acceleration fields are developed through linear Airy's wave theory, and the wave force is computed through Morison's equation (see Figure 4). The CSI SAP2000 automatically defines load cases for the defined wave load patterns. The program provides the option to look at multiple wave crests, but since the waves being looked at have long periods, user only need to look at one wavelength for static loading. Figure 4 shows the wave load pattern definition with an aligned wave. The magnitude of wave load is assigned based on the surface area exposed to a member's wave loading and volume. The wave loads are calculated and applied to the model manually. Once a wave load case is defined, there is no need to assign the wave loads to a member separately, only to provide the Monopod tower with appropriately representative surface areas and volumes. Figure 5 shows the load pattern displaying the resultant velocity of the wave. The wave load distribution over both load cases is compared in Figure 6. Figure 6 (a) wave loads are calculated by CSI SAP2000 module processes automatically, and Figure 6 (b) demonstrates wave load distribution calculated manually by using Morison's equation and applied to members with alternative static load cases. Base Reactions under both wave loading modules and equivalent static wave loads are listed in Table 3. There is a significant difference between both wave loading methods with equal parameters that truly illustrate the difficulties of simulation. A simulation model always abstracts away from the accurate values calculated via Morison's equation, which can affect the member stress rates and internal forces for further dynamic analysis. For the given monopod problem, the wave load distribution can be calculated manually according to Morison's equation, which is seen as Eq. 10. The design parameters could be obtained as $m = 0.095$ and $F_D(z) = 394267.3 \cdot e^{2mz}$, respectively.

Height-wise distribution of joint displacement and moment M3 for a monopod tower under both manual and automatic program-defined wave loads is illustrated in Figure 7. Compared to the manual wave load distribution, the results show that the wave loads calculated by the CSI SAP2000 module processes are too low. Figure 8 depicts the monopod displacement from CSI SAP2000 vs. the real part of SAPOS. The real part of SAPOS, which is related to the drag coefficient, has a minor contribution to wave loading, and in this case, the results are similar to those of CSI SAP2000 in both the displacement pattern and the response ranges (see Figure 8). The contribution of the inertia force component is of major importance here and needs to be reflected in the results. It is known that the contribution of the inertia force component is more dominant, particularly for cylindrical monopod towers with large diameters. The drag and inertia coefficients are defined automatically by default. The drag and inertia force coefficients were taken as per API by the CSI SAP2000 platform [28]. Different results are obtained manually by defining similar input values, implying some problems in the wave load definition module. In addition, changing the inertia coefficient along the Monopod tower does not affect the total wave load pattern, which in turn raises doubts about the correctness of the results.

Table 4: The moment force at the basement

Output Case	Global FX	Global FZ	Global MX	Global MY
Unit	N	N	N-m	N-m
Wave	-106903.59	-191853157	0	-10243336.2
Static Load	-4164332.05	0	0	-372546018

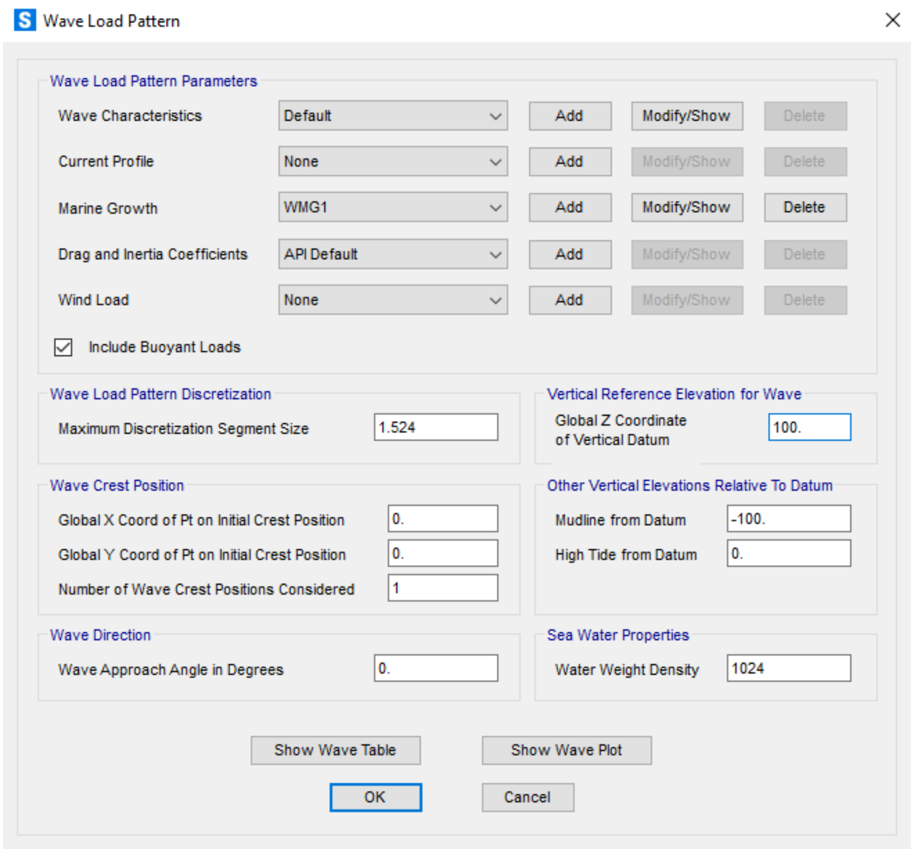

Figure 4. Wave load pattern definition in CSI SAP2000 V.20 for the aligned heading case of wave loading (units in meters) [28].

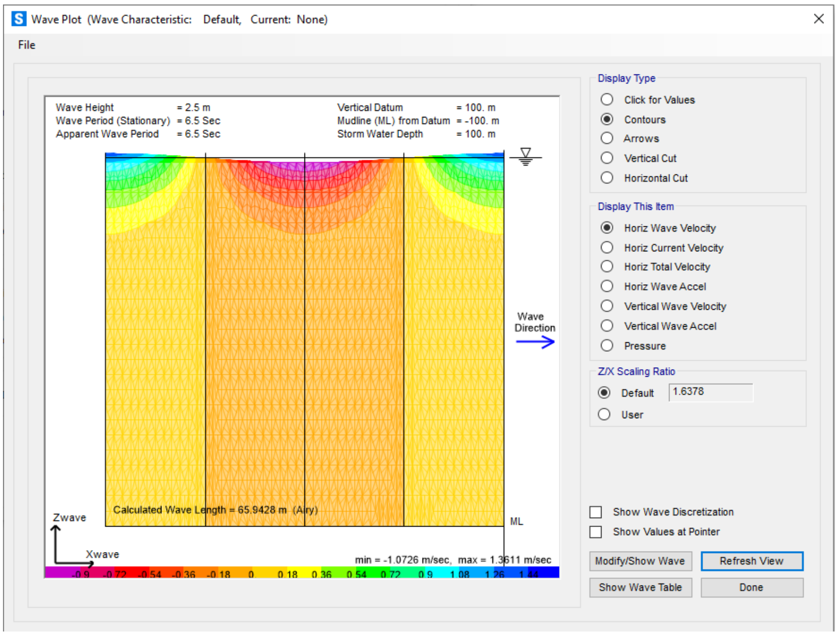

Figure 5. Wave load pattern plot displaying the resultant velocity of the wave in CSI SAP2000 [28].

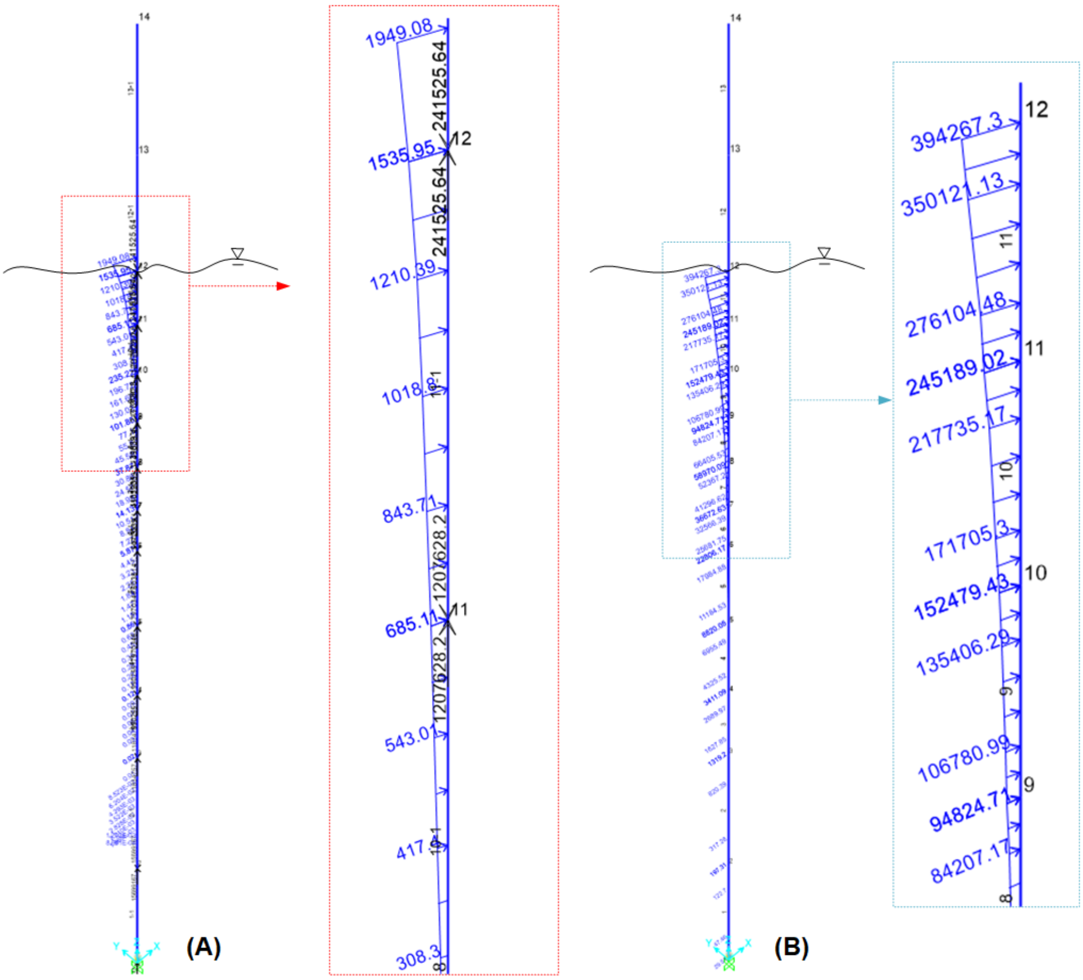

Figure 6. Wave load case applied to a monopod tower: (a) wave loads calculated by CSI SAP2000 module processes; (b) wave load distribution calculated manually using Morison’s equation. (Units are kN).

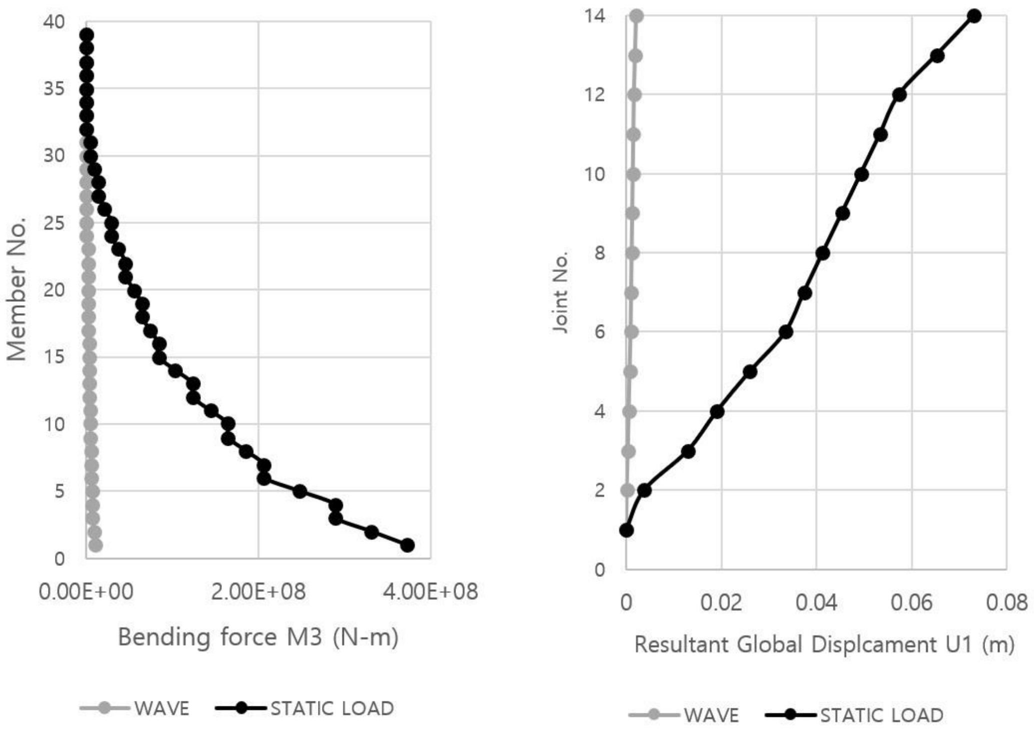

Figure 7. Member bending force M3 and displacement pattern of Monopod tower under program-defined wave loading and static load case calculated manually

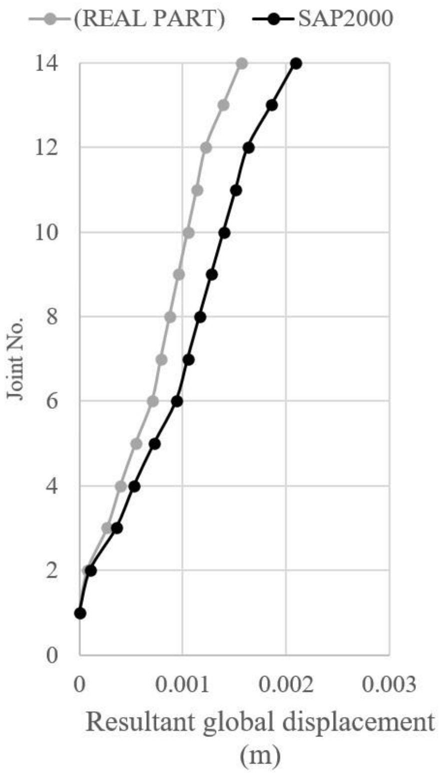

Figure 8. Monopod resultant displacement pattern from SAP2000 vs. SAPOS real part

4.3. Structural Analysis Computer System (SACS) Software

A comprehensive software package called SACS V.12 supports offshore structure analysis, design, and installation (Bentley Systems, 2018) [29]. The monopod tower model refinement phase employs the interactive full-screen graphical user Modeller (PRECEDE) program for hydrodynamic evaluation. The monopod characterizations and primary loads remain constant throughout the evaluation. The environmental loads on a fixed offshore structure are created and computed by SEA STATE using the API 20th edition [2] and several wave loading theories. This module computes the static and dynamic forces within and upon each part of the offshore structure using computer-based operations on environmental and design data provided by the user. The resultant moment forces under Airy's wave loading are plotted in Figure 9. There is a significant difference between the analytical solution and numerical calculated results with equal design parameters that truly demonstrate the simulation's difficulties; a simulation model always abstracts away from the actual conditions. This is one of the essential benefits of simulation, but it also means that the results may only sometimes match the real values.

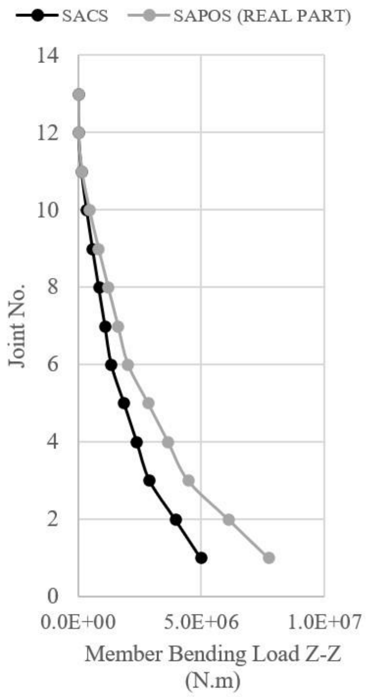

Figure 9. Member bending load under Airy's wave loading from SACS program and SAPOS (Real part)

4.4. ABAQUS Software

Another tool used to investigate wave loading on underwater or partially submerged offshore structures is the ABAQUS/AQUA V.6.14 [30] software, which is used in problems such as the analysis of marine risers and the modelling of offshore piping systems and monopod towers. This module calculates certain rigid elements' drag, buoyancy, and inertia forces. The monopod tower model is generated, and an Airy linear wave load is described, as shown in Table 5. To neglect the wind load, the coefficient value of the wind velocity components is entered as zero. The joint displacement, U1, over the monopod height is illustrated in Figure 10. However, the displacement pattern is similar, but the maximum displacement at the tower tip is obtained as 1.36 m, which is overestimated when compared to the analytical solution and the results of other analysis programs. The displacement pattern is identical, but the displacement demands are overestimated compared to the analytical results.

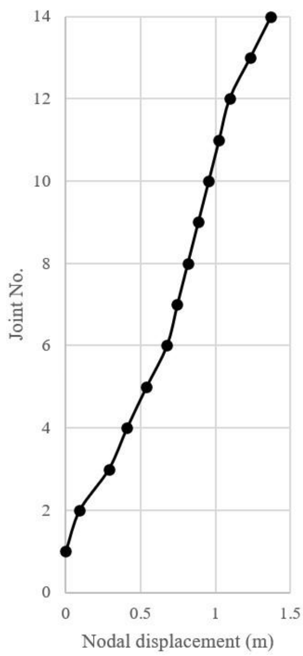

Figure 10. Monopod tower joint displacement distribution, U1, using ABAQUS/Aqua programs [30]

Table 5: Monopod wave loading input file for Abaqus/Aqua

```
*aqua
0,100,9.81,1024
0,0,0,0
0,0,0,100
*wave,type=airy, wave period
1.25,6.5,0,1
*wind
1.225,0.0,0,0,-1
*restart,write,frequency=1
*step
corrent flow
*static
1,1,1e-05, 1
```

5. Results and Discussions

Wave loads dominate the design and performance assessment processes of offshore structures. The finite element-based method is generally adopted for predicting marginal structural response and external loads such as wave loads. However, the results are considered realistic by the users even without an identification process in some cases. This study uses common FE offshore structure analysis platforms to figure out how a simple cylindrical monopod tower will react to a linear Airy's wave. The results are compared with analytical solutions. Because the node displacement generated in a structure is caused by its internal forces and stresses, it is fixed to use the node displacement as the index to evaluate the response of the monopod tower under a static wave load. Another response indicator used to compare findings was bending forces. Utilizing nodal displacement amounts and several numerical approaches of different commercial programs, the author defines the sensitivity of wave forces for default values and various input variables when defining wave load automatically through the wave loading interface module of offshore analysis platforms. The analytical solutions indicate that the maximum shear forces and moments at the bottom for wave number m=0.095 are calculated as V_Max=0.4738732×10^7 N and M_Max=42.3991878×10^7 N·m. Besides, the drag and inertia force coefficients are C_D=10316 and C_M=386.441, respectively. The SOPOS program provides the wave load for the deep-water condition and it has been found that the program can estimate the internal loads with acceptable accuracy. However, in the case of other software (SAPOS, SAP2000, SACS, and ABAQUS), the results do not match very well for the case study. For a more detailed examination of the problem, the wave load is defined automatically via the wave load module in CSI SAP2000 (see Figures 4 and 5). The results are surprisingly underestimated the ranges expected. When one calculated the wave loads manually and performed the static analysis, the displacement demands came out as expected. There is an error in the calculation of the forces resulting from the wave load calculation (see Figure 6). No significant changes in wave loading were seen when the drag and inertia coefficients were changed. The reason for this seems to be that the contribution of the drag coefficient is not taken into consideration. As stated earlier, the inertia coefficient contributes to the wave loading of the cylindrical member with a large diameter. In the following steps, it was shown that the result of CSI SAP2000 is similar in pattern and varies according to the real part response of the SAPOS software regarding the drag coefficient. This supported the view that only the drag coefficient is considered in the calculations (Figure 8). For further investigation, two other commercial FE software products are adopted for wave loading problems. The bending loads show that the load ranges are also around the Real part of the SAPOS results (Figure 9). In solving the problem, the ABAQUS/AQUA module calculates the drag, buoyancy, and inertia forces for certain rigid members. The nodal at the monopod tip reaches 1.36 m, which is very high when compared to analytical solutions.

6. Conclusions

This study presents a wide-ranging analysis of the main contributing factor in the definition of static wave load for cylindrical monopod tower systems. Wave loads significantly impact the design life of offshore structures, such that a realistic estimation of wave loading can affect the overall performance of offshore substructures and the stress level at critical zones. Wave velocity fields are developed through linear Airy's wave theory, and the wave forces are computed through Morison's equation, where the wave load is composed of the drag force and the inertial forces. It is known that the contribution of inertial forces increases with the tabular member's increasing diameter. This is not the case for large-sized cylindrical elements such as monopod towers, as the weight of inertia forces in Morison's equation is negligible for pipe-type components of jacket structures. The simple vertical cylindrical monopod tower with a large diameter is adopted as a case study to compare the static Airy's wave loads of numerical methods with identical analytical solutions. Therefore, only static Airy's wave loads were used to analyze the monopod tower. Other environmental loads, like wind and current loads, were not considered. In this way, it was possible to compare numerical results with analytical solutions. The extreme shear force and maximum static bending moment to which the tower is exposed in deep water conditions are calculated analytically. Commercial FE platforms have been adopted for analyzing monopods under Airy's wave loading. The number of elements and meshing details are the same for all software models. The main results of this study can be listed below:

- Estimating wave loading on offshore structures using FE methods is a contentious issue. And using wave load results without validating them for further analysis could lead to unsafe outcomes. A realistic estimation of internal forces and stress levels can highly affect the performance of offshore structures.

- The wave loading based on Airy's wave theory and Morison's equation is composed of both drag and inertia components. Each contribution of each may also vary with element cross section size. For large-diameter cylindrical members, the contribution of inertia force is dominant. Evaluation of the monopod case shows that the current numerical models may not be able to predict wave loading, mainly when the contribution of the coefficient of inertia to the total instantaneous wave force is dominant.

- As a result of the study, inconsistencies were observed in calculating the inertia load of commercial programs. The shear forces and moment reactions are compared. The difference arises from the inclusion of the inertia force component contribution to the wave loads. The results of the SAPOS program demonstrated good agreement with the analytical solution among the examined FE software packages.

Article Information Form

Funding

The author (s) has no received any financial support for the research, authorship or publication of this study.

Authors’ Contrtibution

The authors contributed equally to the study.

The Declaration of Conflict of Interest/Common Interest

No conflict of interest or common interest has been declared by the authors.

The Declaration of Ethics Committee Approval

This study does not require ethics committee permission or any special permission.

The Declaration of Research and Publication Ethics

The authors of the paper declare that they comply with the scientific, ethical and quotation rules of SAUJS in all processes of the paper and that they do not make any falsification on the data collected. In addition, they declare that Sakarya University Journal of Science and its editorial board have no responsibility for any ethical violations that may be encountered, and that this study has not been evaluated in any academic publication environment other than Journal of Innovative Science and Engineering.

References

[1] Chakrabarti, S. (2005). Handbook of offshore engineering. 1st ed.1-2, *Oxford: El-Sevier Applied Science.*

[2] API RP 2A-WSD. (2007) Recommended Practice for Planning, Designing and Constructing Fixed Offshore Platforms - Working Stress Design - Twenty-First Edition, Errata and Supplement 3.

[3] Abdel Raheem Sh, E., Abdel Aal E, M. A., Abdel Shafy A. G. A. and Abdel Seed, F. K. (2012). Nonlinear analysis of offshore structures under wave loadings, *Proceedings of the 15th World Conference on Earthquake Engineering*-15WCEE, 24–28.

[4] Raheem, A. E. S. (2013). Nonlinear response of fixed jacket offshore platform under structural and wave loads, Coupled Systems Mechanics, 2: 111–126. DOI: 10.12989/csm.2013.2.1.111

[5] A storm at sea from the view of an oil rig, URL: https://www.reddit.com/r/pics/comments/13q5u9/a_storm_at_sea_from_the_view_of_an_oil_rig/

[6] Witz, J. Lyons, G. Patel, M.H. and Brown, D. (1994). Advanced Offshore Engineering, Offshore Engineering Handbook Series. *Bentham Press*, London, UK.

[7] Karadeniz, H. (2013). Stochastic Analysis of Offshore Steel Structures. *An Analytical Appraisal*, *Springer Series in Reliability Engineering*. DOI:10.1007/978-1-84996-190-5

[8] Boccotti, P. (2015). Wave mechanics and wave loads on marine structures, in: Butterworth-Heinemann publication, Waltham, MA 02451, USA, ISBN: 978-0-12-800343-5, 978–978.

[9] Linton, C.M. and Evans, D.V. (1990). The interaction of waves with arrays of vertical circular cylinders, J. Fluid Mech, 215: 549-569. DOI: https://doi.org/10.1017/S0022112090002750

[10] Kriebel, D.L. (1990). Nonlinear wave interaction with a vertical circular cylinder. Part I: *Diffraction Theory*, *Ocean Engineering*, 17(4): 345–377. https://doi.org/10.1016/0029-8018(90)90029-6

[11] Kriebel, D.L. (1992). Nonlinear wave interaction with a vertical circular cylinder. part II: *Wave Run-Up*, *Ocean Engineering*, 19(1):75-99. https://doi.org/10.1016/0029-8018(92)90048-9

[12] Zhu, S. (1993). Diffraction of short-crested waves around a circular cylinder, *Ocean Engineering*, 20: 389–407, https://doi.org/10.1016/0029-8018(93)90003-Z

[13] Vugts, J.H. Tempel, J.V.D. and Schrama, E.A. (2001). Hydro-dynamic loading on Monotower support structures for preliminary design. *Interfaculty Offshore Technology, Faculty of Civil Engineering and Geosciences*, Delft University of Technology.

[14] Wilson, J.F. (2003). Dynamics of Offshore Structures, *John Wiley & Sons, Inc*, United States of America. ISBN: 978-0-471-26467-5.

[15] Harish, N. Sukomal, M. Shanthala, B. and Subba, R. (2010). Analysis of offshore jacket platform, Natl. Conf. on Sustainable Water Resources Management - SWARM, 7–9.

[16] Karadeniz, H. Togan, V. and Vrouwenvelder, T. (2008a). Optimization of steel monopod offshore-towers under probabilistic constraints, *Proceedings of the International Mechanical Engineering Congress and Exposition*, Boston, USA.

[17] Karadeniz, H. Togan, V. and Vrouwenvelder, T. (2008b). Reliability based optimization of steel monopod offshore towers, *Proceedings of the 27th International Conference on Offshore Mechanics and Arctic Engineering*, Estoril, Portugal.

[18] Slåke, T. (2016). Analysis of Jacket type fixed platforms- Effect of various mass modelling approaches for Topsides on structural response, MASTER Thesis, University of Stavanger, Stavanger, Stavanger, Norway.

[19] Morison, J.R. Brien, M.P. WJohnson, J. and Schaaf, S.A. (1950). The force exerted by surface wave on piles, *Petroleum Transactions, American Institute of Mining Engineers*, 189:149-154. DOI:10.2118/950149-G

[20] Mendes, A.C. Kolodziej, J.A. and Correia, H.J.D. (2004). Numerical modelling of wave-current loading on offshore jacket structures, *Transactions on the Built Environment*, 71. DOI: 10.2495/FSI030091

[21] Lipsett, A.W. (1986). A perturbation solution for nonlinear structural response to oscillatory flow, *Applied Ocean Research*, 8(4):183-189. https://doi.org/10.1016/S0141-1187(86)80035-9

[22] Gudmestad, O.T. and Moe, G. (1996). Hydrodynamic Coefficients for Calculation of Hydrodynamic Loads on Offshore Truss Structures, Marine Structures, 9:23. 0951-8339(95)00023-23-2

[23] Sunder, S. and Connor, J. (1981). Sensitivity analyses for steel jacket offshore platforms, *Applied Ocean Research*, 3(1):19-28. DOI:10.1016/0141-1187(81)90081-X

[24] Chandrasekaran, S. Jain, A.K. and Chandak, N.R. (2004). Technical note: Influence of hydrodynamic coefficients in the response behavior of triangular TLPs in regular waves, Ocean Engineering, 31:2319-2342. https://doi.org/10.1016/j.oceaneng.2004.06.005

[25] Gücüyen, E. Erdem, R.T. and Gökkuş, Ü. (2012). Irregular wave effects on dynamic behavior of piles, *Arabian J. Sci. Eng. King Fahd University of Petroleum and Minerals*. DOI 10.1007/s13369-012-0428-6.

[26] Edvardsen, K. (2015). Forces on simplified offshore structures according to different wave models, Norway.

[27] Karadeniz, H. (1989). Advanced stochastic analysis program for offshore structures - Theoretical outline and the user's manual of SAPOS, Report, *Dept. of Civil Engineering, Delft University of Technology*, Delft, Netherland.

[28] CSI Analysis Reference Manual. (2014). CSI analysis reference manual for SAP2000 *Version 16; Computers & Structures Inc*. (CSI): Walnut Creek, CA, USA.

[29] SACS (2009). Version 12, EDI, Soft-ware Manual Version 7.

[30] Abaqus theory manual. (2004). Version 6.14-1 Hibbitt. *Karlsson and Sorensen, Inc*. Pawtucket, RI.

[31] ANSYS (2016). AQWA user's manual release 17.0. ANSYS Inc.: Canonsburg, PA, USA.

[32] Cermelli, C. Aubault, A. Roddier, D. and Mccoy, T. (2010). Qualification of a Semi-Submersible Floating Foundation for Multi-Megawatt Wind Turbines, *Offshore Technology Conference, Offshore Technology Conference*, 1–15.

[33] Computers, Structures, Inc, (2011). Automatic Wave Loads Technical Note Wave Load Overview. *Computers and Structures*, Inc, Berkeley, CA.

[34] Doman, A.C. (2014). Three-Dimensional equivalent static analysis and design methodology of a reinforced concrete floating offshore wind turbine platform, *California State University, Sacramento*.

[35] Lai, W.J. Lin, Ch.Y. Huang, Ch.Ch. and Lee, R.M. (2016). Dynamic Analysis of Jacket Substructure for Offshore Wind Turbine Generators under Extreme Environmental Conditions, *Appl. Sci*, 6:307. doi:10.3390/app6100307

[36] Kazemi Daliri, A. (2017). Evaluation of using new materials in offshore jacket structures and risers, PhD. *Dissertation, İstanbul Aydin University,* Istanbul, Turkey.

[37] Noorzaei, J. Bahrom, S. I. Jaafar, M.S. Abdul, W. Thanoon, M. and Mohammad, Sh. (2005). Simulation of Wave and Current Forces on Template Offshore Structures, *Suranaree J. Sci. Technol*, 12(3):193-210.

[38] Ishwarya, S. (2016). Nonlinear static and dynamic analyses of jacket-type offshore platform, *Anna University*, Chennai.

[39] Karadeniz, H. (1996). Spectral Analysis Program for Offshore Structures (SAPOS), Response calculation and fatigue damage estimates, *Proc. of the 2nd Int. Conference in Civil Engineering on Computer Applications*, Research and Practice, ICCE-96, 1:339-349.

[40] Yaylacı, M. (2007). Applications of offshore Structure and Explicated of Design Parameters, *Karadeniz Technical University*, Trabzon, Turkey.

[41] Mc Namara, J.F. Gilroy, J.P. Sorensen, E.P. and Hibbitt, H.D. (1985). ABAQUS/AQUA application to offshore risers and pipelines, *Maritime Simulation, Proceedings of the First Intercontinental Symposium*, Springer.

[42] Kuntiyawichai, K. and Chucheepsakul, S. (2004). Analysis of offshore structures subjected to various types of sea wave, *Proceedings of OMAE04, 23rd International Conference on Offshore Mechanics and Arctic Engineering, Vancouver*, Canada.

[43] Huizer, C.O. (2017). Modelling loads of steady current and waves with Abaqus, Aqua. URL: Url-2<https://info.simuleon.com/blog/modelling-loads-of-steady-current-and-waves-with-abaqus-aqua

[44] Das, B. and Janardhan, P. (2017). Model Development and Load Analysis of Offshore Jacket Structure using SAP2000, *International Journal for Research in Applied Science and Engineering Technology (IJRASET)*, 5:1482-1493. doi:10.22214/ijraset.2017.4263

[45] Dağlı, B. Y. Yiğit, M.E. and Gökkuş, U. (2017). Behaviour of large cylindrical offshore structures subjected to wave loads, *TEM Journal*, 6(3):550-557. DOI:10.18421/TEM63-16

[46] Lamb H. (1993) Hydrodynamics. *Cambridge University Press*, Cambridge.

[47] Maccamy, R.C. and Fuchs, R.A. (1954). Wave Forces on Piles: A Diffraction Theory, Army Corps of Engineers, *Beach Erosion Board. U.S. Beach Erosion Board*, ech. Memo No. 69.

[48] Sarpkaya, T. and Isaacson, M. (1981). Diffraction theory is reviewed in Mechanics of Wave Forces on Offshore Structures, Van Nostrand Reinhold Co.

[49] Det Norske Veritas - DNV (1977). Result for the Design, *Construction and Inspection of Offshore Structures*, Oslo, (Reprint with correction 1981). http://www.dnv.com

[50] Sawaragi, T. (1995). Coastal engineering- waves, beaches, wave-structure interaction. *Elsevier, Amsterdam.*

[51] Butterfield, S. Musial, W. Jonkman, J. Sclavounos, P. and Wayman, L. (2007). Engineering Challenges for Floating Offshore Wind Turbines, Golden, Colorado: National Renewable Energy Laboratory